JOURNAL OF THEORETICAL
AND APPLIED MECHANICS
4, **38**, 2000

AN ALGORITHM OF A FAMILY OF 3D-BASED, SOLID-TO-SHELL TRANSITION, *hpq*/*hp*-ADAPTIVE FINITE ELEMENTS

GRZEGORZ ZBOIŃSKI
WIESŁAW OSTACHOWICZ

Institute of Fluid Flow Machinery Polish Academy of Sciences
e-mail: zboi@imppan.imp.pg.gda.pl

The basic information on an algorithm of a family of new triangular-prism, 3D-based, *hpq*/*hp*-adaptive, solid-to-shell transition finite elements has been presented in the paper, where h, p and q denote an averaged size as well as longitudinal and transverse orders of approximation of the elements, respectively. Novelty of the elements consists in application of *hpq*- and *hp*-approximations in solid and shell parts of the elements, respectively. In that context, crucial parts of the algorithm such as: hierarchical shape functions, modification of the stiffness and nodal forces of the shell part of the elements, and constrained *hpq*/*hp*-approximation are elucidated. Usefulness of the elements for modelling and analysis of complex structures is proved by a numerical example.

Key words: finite elements, solids, shells, transition zones, adaptivity

1. Introduction

Recent developments in *hpq*- and *hp*-approximations and in the corresponding finite element methods have become a strong impulse for revising the possibilities of application of adaptive, solid and shell finite elements to an analysis of plates, shells and solid bodies. In that context we should mention the work by Demkowicz et al. (1989) on three-dimensional *hp* (or *hpp*) finite element approximations applied to 3D-elasticity problems. Note that *hpq*-approximation being a specific case of *hpp*-approach can be used also for thick and moderately thick shells. The corresponding hexahedral finite elements were proposed earlier by Szabo and Sahrmann (1988) while the triangular-prism elements were described by Zboiński (1997) quite recently. On the other

hand, we have works concerning two-dimensional *hp*-approximations for thin or moderately thick shell and plate problems. Some theoretical considerations are given by Babuška and Li (1992). The corresponding, exemplary quadrilateral shell finite elements can be found in Della Croce and Scapolla (1992) and in Chinosi et al. (1998). As an alternative 3D-based, triangular-prism, Reissner-Mindlin shell element was elaborated by Zboiński (1994). Still one more approach proposed by Oden and Cho (1996) utilizes quadrilateral shell elements based on *hpq*-approximation and hierarchical models of thin, moderately thick and thick shells and plates. A similar idea is also applied in the *hpq* hierarchical elements by Actis et al. (1999). It is not our intention to extend the above list of exemplary papers. It is worth noting, however, that:

- The works by predecessors concern solid, shell or plate bodies separately because of assignment of the above mentioned approaches to the specific, different models and geometries
- The specific character of the above mentioned approaches results in different formulation of the corresponding finite element approximations with incompatible degrees of freedom (DOFs) applied
- As a result, modelling and general analysis of complex structures consisting of solid and thin- or thick-walled parts as well as of transition zones is not possible, or at least very difficult, either with each of the above approaches or by means of all of them together.

In order to overcome this difficulty we utilize a family of original, compatible 3D-solid, 3D-based shell and 3D-based solid-to-shell transition elements elaborated by Zboiński and Demkowicz (1994), Zboiński (1994) and Zboiński and Ostachowicz (1995), respectively. These elements are based on *hpq*-, *hp*- and *hpq*/*hp*-approximations, and are assigned for consistent modelling and adaptive analysis of solid, shell and transition parts of complex structures.

The paper focuses on algorithms of solid-to-shell transition elements. This idea is not new. It was proposed by Surana (1980) in the context of classical (non-adaptive) finite elements. The elements proposed here (Zboiński and Ostachowicz, 1995, 1999a) take advantage of this idea and of 3D-based non-adaptive shell elements introduced by Zboiński (1992). Apart from their adaptive character, novelty of our elements in comparison to classical ones lies in the followig facts:

- Adaptive character of the proposed elements needs introduction of hierarchical shape functions defined independently in vertices, on edges and faces, and in the interior of the element, in order to enable the adaptation process

- 3D approach is proposed for element formulation which results in application of three-dimensional DOFs instead of shell DOFs in the shell part of the elements
- Definition of local, normal and tangent directions in any point of the shell part of the elements conforms to shell theory, i.e. corresponds with the mid-surface instead of surfaces of constant normalized longitudinal coordinates applied in the case of classical elements
- The solid part of the presented elements, which comprises most of the element nodes, except those constituting the shell part and belonging to edges and faces, are defined in agreement with 3D-elasticity theory in comparison to the nodes of almost equal shell and solid parts of the classical elements, which conform to the shell theory.

2. An algorithm of the elements

The presented parts of the algorithm are limited to crucial aspects, while the full algorithm is given by Zboiński and Ostachowicz (1999a,b). An emphasis is put on details describing adaptive character of the elements, which are not present in the case of classical elements. Some other differences between the proposed and classical elements are also shown.

2.1. Normalized geometry of the elements

In order to connect solid and shell parts of any complex structure, which are modelled by 3D-solid and 3D-based shell elements, we need to introduce four transition elements. In the first of them (I), the shell part of the element consists of two vertex nodes $\boldsymbol{a}_1$, $\boldsymbol{a}_4$ of one vertical edge $\overline{\boldsymbol{a}_1\boldsymbol{a}_4}$, in the second (II) this part includes four vertex nodes: $\boldsymbol{a}_1$, $\boldsymbol{a}_2$, $\boldsymbol{a}_4$, $\boldsymbol{a}_5$ and two mid-edge nodes: $\boldsymbol{a}_7$, $\boldsymbol{a}_{10}$ of one side $\square\boldsymbol{a}_1\boldsymbol{a}_2\boldsymbol{a}_5\boldsymbol{a}_4$, in the third case (III) the shell part consists of the nodes of two sides $\square\boldsymbol{a}_1\boldsymbol{a}_2\boldsymbol{a}_5\boldsymbol{a}_4$ and $\square\boldsymbol{a}_2\boldsymbol{a}_3\boldsymbol{a}_6\boldsymbol{a}_5$, while for the fourth (IV) case we have three sides. The geometry of the master elements defined by the normalized coordinates ξ_1, ξ_2 and ξ_3 (changing from 0 to 1) is shown in Fig.1.

2.2. Hierarchical shape functions of the elements

If we introduce functions ψ_i, $i = 1,3$; ψ_j^k, $j = 1,3$, $k = 1,...,N_j - 1$; ψ_7^k, $k = 1,...,(N_4 - 2)(N_4 - 1)/2$ denoting vertex, mid-edge and middle node

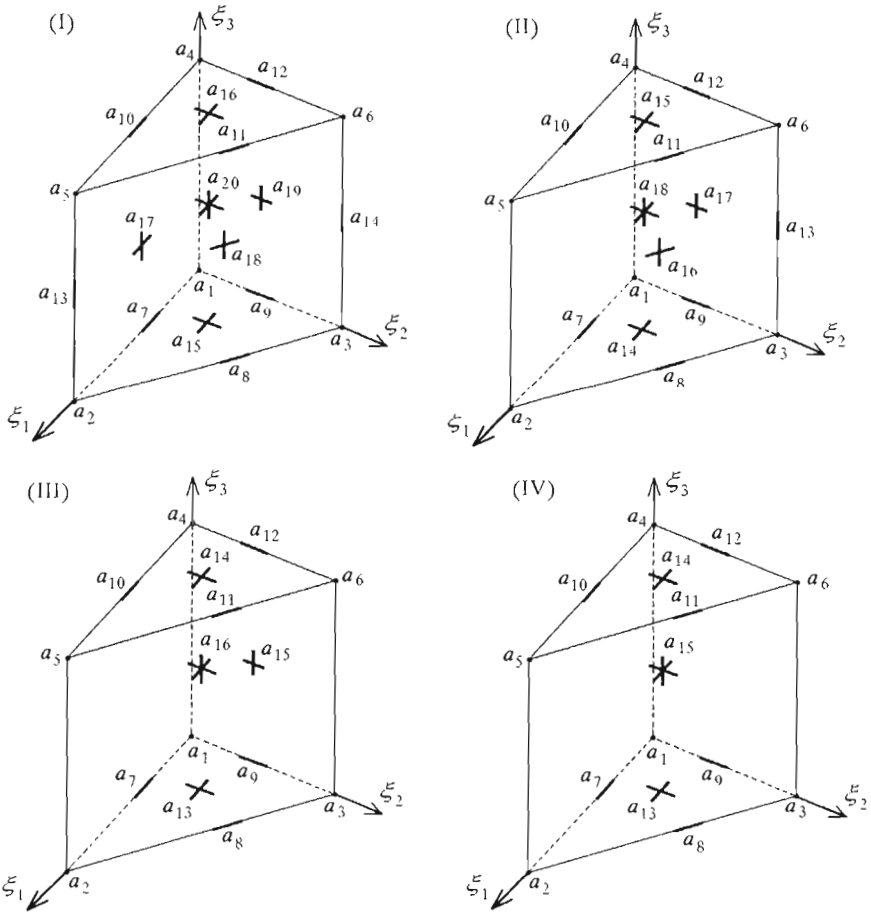

Fig. 1. Cases (I)-(IV) of adaptive transition elements

shape functions (defined independently within $\xi_1\xi_2$-plane) of a 2D triangular master element of order (of higher-order nodes) expressed by the vector $[N_1, N_2, N_3, N_4]$, and functions ϕ_1, ϕ_2; ϕ_3^l, $l = 1, 2, ..., M$ being shape functions (defined independently along ξ_3) corresponding to vertices and interior of 1D master element (of order of the middle node equal M), then 3D hierarchical shape functions can be obtained as tensor products of 2D and 1D shape functions.

The 2D shape functions mentioned above which correspond with the following nodes of the master triangle take the form of:

— vertex nodes

$$\psi_i = \lambda_i \qquad i = 1,2,3 \tag{2.1}$$

— the first mid-edge node

$$\psi_4^k = \frac{\prod\limits_{j=0,j\neq k}^{N_1}\left[\left(1-\frac{j}{N_1}\right)\lambda_2 - \frac{j}{N_1}\lambda_1\right]}{\prod\limits_{j=0,j\neq k}^{N_1}\left[\left(1-\frac{j}{N_1}\right)\frac{k}{N_1} - \frac{j}{N_1}\left(1-\frac{k}{N_1}\right)\right]} \qquad k = 1,...,N_1-1 \tag{2.2}$$

with formulas for the shape functions ψ_5^k, ψ_6^k of the next two mid-edge nodes obtained by replacing indices 1, 2 in Eq (2.2) with 2, 3 and 3, 1, respectively

— middle node

$$\psi_7^k = \frac{\prod\limits_{m=0}^{g-1}\left(\lambda_1 - \frac{m}{N_4}\right)\prod\limits_{n=0}^{h-1}\left(\lambda_2 - \frac{n}{N_4}\right)\prod\limits_{r=0}^{j-1}\left(\lambda_3 - \frac{r}{N_4}\right)}{\prod\limits_{m=0}^{g-1}\left(\frac{g}{N_4} - \frac{m}{N_4}\right)\prod\limits_{n=0}^{h-1}\left(\frac{h}{N_4} - \frac{n}{N_4}\right)\prod\limits_{r=0}^{j-1}\left(\frac{j}{N_4} - \frac{r}{N_4}\right)} \tag{2.3}$$

where $g+h+j = N_4$, $1 \leqslant g,h,j \leqslant N_4$ and consecutive values of $k = 1,...,(N_4-2)(N_4-1)/2$ correspond to threesomes g,h,j in which the values of j, h and g are consecutively increased.

Note that we use so-called affine (or area) coordinates λ_1, λ_2, λ_3 in (2.1)-(2.3), which can be expressed through normalized coordinates ξ_1, ξ_2 with simple formulas $\lambda_1 = 1-\xi_1-\xi_2$, $\lambda_2 = \xi_1$ and $\lambda_3 = \xi_2$. It is worth noting that the form of the shape functions for the mid-edge nodes is an original one and different from the form proposed by the predecessors.

The form of the mentioned 1D shape functions corresponding with two vertex nodes and one middle node are defined as follows:

— vertex nodes

$$\phi_1 = 1-\xi_3 \qquad \phi_2 = \xi_3 \tag{2.4}$$

— middle node

$$\phi_3^l = \frac{\prod\limits_{j=0,j\neq l}^{M-1}\left(\xi_3 - \frac{j}{M}\right)(1-\xi_3)}{\prod\limits_{j=0,j\neq l}^{M-1}\left(\frac{l}{M} - \frac{j}{M}\right)\left(1-\frac{l}{M}\right)} \qquad l = 1,...,M-1 \tag{2.5}$$

Proper multiplication of 1D and 2D shape functions leads to the following 3D shape functions, for:

— lower and upper vertex nodes

$$\begin{aligned} \chi_i &= \psi_i \phi_1 \qquad && i = 1,2,3 \\ \chi_{3+i} &= \psi_i \phi_2 \qquad && i = 1,2,3 \end{aligned} \tag{2.6}$$

— lower and upper horizontal mid-edge nodes

$$\begin{aligned} \chi_{6+j,k} &= \psi^k_{3+j} \phi_1 \qquad && j = 1,2,3 \qquad k = 1,...,N^e_j - 1 \\ \chi_{9+j,k} &= \psi^k_{3+j} \phi_2 \qquad && j = 1,2,3 \qquad k = 1,...,N^e_{3+j} - 1 \end{aligned} \tag{2.7}$$

— optional vertical mid-edge nodes $(i = i^p, ..., i^k)$

$$\chi_{12+i,l} = \psi_{j_i} \phi^l_3 \qquad l = 1,..., M^e_{j_i} - 1 \tag{2.8}$$

where for (I): $i^p = 1$, $i^k = 2$, $(j_1, j_2) \in \{(2,3),(3,1),(1,2)\}$ and for (II): $i^p = i^k = 1$, $j_1 \in \{3,1,2\}$

— lower and upper mid-base nodes

$$\begin{aligned} \chi_{I^b+1,k} &= \psi^k_7 \phi_1 \qquad && k = 1,..., \frac{(N^b_1 - 2)(N^b_1 - 1)}{2} \\ \chi_{I^b+2,k} &= \psi^k_7 \phi_2 \qquad && k = 1,..., \frac{(N^b_2 - 2)(N^b_2 - 1)}{2} \end{aligned} \tag{2.9}$$

where for (I): $I^b = 14$, (II): $I^b = 13$, (III) and (IV): $I^b = 12$

— optional mid-side nodes: $(i = i^a, ..., i^z)$

$$\chi_{I^s+i,m} = \psi^k_{3+j_i} \phi^l_3 \qquad \begin{cases} k = 1,..., (N^s_{j_i} - 1) \\ l = 1,..., (M^s_{j_i} - 1) \\ m = (k-1)(M^s_{j_i} - 1) + l \end{cases} \tag{2.10}$$

where for (I): $I^s = 16$, $i^a = 1$, $i^z = 3$, $(j_1, j_2, j_3) \in \{(1,2,3)\}$, for (II): $I^s = 15$, $i^a = 1$, $i^z = 2$, $(j_1, j_2) \in \{(2,3),(3,1),(1,2)\}$, and for (III): $I^s = 14$, $i^a = i^z = 1$, $j_1 \in \{3,1,2\}$

— middle node

$$\chi_{I^c,m} = \psi^k_7 \phi^l_3 \qquad \begin{cases} k = 1,..., \dfrac{(N^c - 2)(N^c - 1)}{2} \\ l = 1,..., (M^c - 1) \\ m = (k-1)(M^c - 1) + l \end{cases} \tag{2.11}$$

where for (I): $I^c = 20$, for (II): $I^c = 18$, for (III): $I^c = 16$, while for (IV): $I^c = 15$.

Note that N^e_j, $j = 1,2,..,6$, $M^e_{j_i}$, N_1, N_2, $(N^s_{j_i}, M^s_{j_i})$, (N^c, M^c) denote orders of approximation of horizontal and vertical edge nodes, base and side nodes, and middle node of the elements.

2.3. Displacement fields of the transition elements

The total interpolant of a displacement field of the transition elements, $\boldsymbol{u} = \boldsymbol{u}(\boldsymbol{\xi})$, describing displacements $\boldsymbol{u} = \mathrm{col}[u_1, u_2, u_3]$ of any point of the elements is a sum of four component interpolants (interpolating functions)

$$\boldsymbol{u}(\boldsymbol{\xi}) = \boldsymbol{u}^1(\boldsymbol{\xi}) + \boldsymbol{u}^2(\boldsymbol{\xi}) + \boldsymbol{u}^3(\boldsymbol{\xi}) + \boldsymbol{u}^4(\boldsymbol{\xi}) \tag{2.12}$$

The linear (vertex nodes) interpolant $\boldsymbol{u}^1(\boldsymbol{\xi})$ can be defined as a sum of products of the local degrees of freedom $\boldsymbol{q}_i$, $i = 1, .., 6$ at vertex nodes and the corresponding shape functions

$$\boldsymbol{u}^1(\boldsymbol{\xi}) = \sum_{i=1}^{6} \chi_i(\boldsymbol{\xi}) \boldsymbol{q}_i \tag{2.13}$$

where these DOFs are defined as $\boldsymbol{q}_i = \mathrm{col}[q_{1,i}, q_{2,i}, q_{3,i}]$.

The mid-edge node interpolant $\boldsymbol{u}^2(\boldsymbol{\xi})$ is defined as a sum of products of the local degrees of freedom $\boldsymbol{q}_{6+i,k}$, $i = 1, ..., 6$ and $\boldsymbol{q}_{12+i,l}$, $i = i^p, ..., i^k$ at the horizontal and optional vertical mid-edge nodes, respectively, and the appropriate shape functions

$$\boldsymbol{u}^2(\boldsymbol{\xi}) = \sum_{i=1}^{6} \sum_{k=1}^{N_i^e - 1} \chi_{6+i,k}(\boldsymbol{\xi}) \boldsymbol{q}_{6+i,k} + \sum_{i=i^p}^{i^k} \sum_{l=1}^{M_{j_i}^e - 1} \chi_{12+i,l}(\boldsymbol{\xi}) \boldsymbol{q}_{12+i,l} \tag{2.14}$$

where vectors of the mentioned degrees of freedom are

$$\boldsymbol{q}_{6+i,k} = \mathrm{col}[q_{1,6+i,k}, q_{2,6+i,k}, q_{3,6+i,k}]$$
$$\boldsymbol{q}_{12+i,l} = \mathrm{col}[q_{1,12+i,l}, q_{2,12+i,l}, q_{3,12+i,l}]$$

and counters i^p, i^k, j_i are the same as in the previous sections.

The next, mid-side nodes interpolant of displacements $\boldsymbol{u}^3(\boldsymbol{\xi})$ is defined analogously by multiplication of the proper local displacement-type DOFs $\boldsymbol{q}_{I^b+i,k}$, $i = 1, 2$ and $\boldsymbol{q}_{I^s+i,m}$, $i = i^a, ..., i^z$ at the base nodes and optional mid-side nodes and the corresponding shape functions

$$\boldsymbol{u}^3(\boldsymbol{\xi}) = \sum_{i=1}^{2} \sum_{k=1}^{(N_i^b-2)(N_i^b-1)/2} \chi_{I^b+i,k}(\boldsymbol{\xi}) \boldsymbol{q}_{I^b+i,k} + \sum_{i=i^a}^{i^z} \sum_{m=1}^{(N_{j_i}^s-1)(M_{j_i}^s-1)} \chi_{I^s+i,m}(\boldsymbol{\xi}) \boldsymbol{q}_{I^s+i,m} \tag{2.15}$$

where the local degrees of freedom are defined by

$$\boldsymbol{q}_{I^b+i,k} = \mathrm{col}[q_{1,I^b+i,k}, q_{2,I^b+i,k}, q_{3,I^b+i,k}]$$
$$\boldsymbol{q}_{I^s+i,m} = \mathrm{col}[q_{1,I^s+i,m}, q_{2,I^s+i,m}, q_{3,I^s+i,m}]$$

and where the quantities I^b, I^s, i^a, i^z, j_i are determined as previously.

The middle node interpolant of displacemnts $\boldsymbol{u}^4(\boldsymbol{\xi})$ can be calculated again through multiplication of the proper local degrees of freedom $\boldsymbol{q}_{I^c,m}$ and the corresponding shape functions

$$\boldsymbol{u}^4(\boldsymbol{\xi}) = \sum_{m=1}^{(N^c-2)(N^c-1)(M^c-1)/2} \chi_{I^c,m}(\boldsymbol{\xi})\boldsymbol{q}_{I^c,m} \tag{2.16}$$

where the local degrees of freedom are

$$\boldsymbol{q}_{I^c,m} = \mathrm{col}[q_{1,I^c,m}, q_{2,I^c,m}, q_{3,I^c,m}]$$

and quantity I^c is defined in the previous section.

2.4. Stiffness modification within a shell part of the elements

The starting point is an element equilibrium equation $\mathbf{k}\boldsymbol{q} = \boldsymbol{f}$, where $\mathbf{k}$ is an element stiffness matrix conforming to the 3D-elasticity theory, while $\boldsymbol{f}$ and $\boldsymbol{q}$ denote element nodal force and displacement DOF vectors. In order to make the shell part of the elements compatible with the shell theory and thus to enable the connection between elements of different models, we introduce within this part the plane strain assumption. Its introduction consists of five steps:

- Replacement of the global DOFs $\boldsymbol{q}$ with generalized DOFs $\boldsymbol{q}^I$ defined as sums or differences of global DOFs of the top and buttom surfaces, that leads to the relation

$$\mathbf{k}^I\boldsymbol{q}^I = \boldsymbol{f}^I \tag{2.17}$$

where $\boldsymbol{q}^I$ consists of the blocks

$$\begin{aligned}
&\boldsymbol{q}^I_{j_i} = \tfrac{1}{2}(\boldsymbol{q}_{j_i} + \boldsymbol{q}_{3+j_i}) && \boldsymbol{q}^I_{3+j_i} = \tfrac{1}{2}(\boldsymbol{q}_{j_i} - \boldsymbol{q}_{3+j_i}) && i = i^u, ..., i^w\\
&\boldsymbol{q}^I_{j_i} = \boldsymbol{q}_{j_i} && \boldsymbol{q}^I_{3+j_i} = \boldsymbol{q}_{3+j_i} && i = i^p, ..., i^k\\
&\boldsymbol{q}^I_{6+j_i} = \tfrac{1}{2}(\boldsymbol{q}_{6+j_i} + \boldsymbol{q}_{9+j_i}) && \boldsymbol{q}^I_{9+j_i} = \tfrac{1}{2}(\boldsymbol{q}_{6+j_i} - \boldsymbol{q}_{9+j_i}) && i = i^b, ..., i^d\\
&\boldsymbol{q}^I_{6+j_i} = \boldsymbol{q}_{6+j_i} && \boldsymbol{q}^I_{9+j_i} = \boldsymbol{q}_{9+j_i} && i = i^a, ..., i^z\\
&\boldsymbol{q}^I_i = \boldsymbol{q}_i && i = 13, 14, ..., I^c &&
\end{aligned}$$

and where i_p, i_k, i_a, i_z are defined as previously, while i_u, i_w, i_b, i_d depend on the element type (I)-(IV), i.e.

– for (I)

$$i^u = i^w = 1 \qquad j_1 \in \{1,2,3\}$$
$$i^p = 1 \qquad i^k = 2 \qquad (j_1, j_2) \in \{(2,3),(3,1),(1,2)\}$$

– for (II)

$$i^u = 1 \qquad i^w = 2 \qquad (j_1, j_2) \in \{(1,2),(2,3),(3,1)\}$$
$$i^b = i^d = 1 \qquad j_1 \in \{1,2,3\}$$

– for (III)

$$i^u = 1 \qquad i^w = 3 \qquad (j_1, j_2, j_3) \in \{(1,2,3)\}$$
$$i^b = 1 \qquad i^d = 2 \qquad (j_1, j_2) \in \{(1,2),(2,3),(3,1)\}$$

– for (IV)

$$i^u = 1 \qquad i^w = 3 \qquad (j_1, j_2, j_3) \in \{(1,2,3)\}$$
$$i^b = 1 \qquad i^d = 3 \qquad (j_1, j_2, j_3) \in \{(1,2,3)\}$$

- Transformation of the global direction of the generalized DOFs to local directions (two directions tangent and one normal to the mid-surface of the shell part of the elements) with transformation matrix $\boldsymbol{\lambda}$ such that $\boldsymbol{q}^I = \boldsymbol{\lambda}\boldsymbol{q}^{II}$

$$\boldsymbol{\lambda}^\top \mathbf{k}^I \boldsymbol{\lambda} \boldsymbol{q}^{II} = \boldsymbol{\lambda}^\top \boldsymbol{f}^I \tag{2.18}$$

that formally leads to $\mathbf{k}^{II}\boldsymbol{q}^{II} = \boldsymbol{f}^{II}$

- Imposing constraints of constant normal displacements in mid-surface edge and vertex points of coordinates $\boldsymbol{\xi}_{l,m} = (\xi_{1,l,m}, \xi_{2,l,m}, \frac{1}{2})$, the points of which are numbered with counters l and m such that for the edges $l = 9 + j_i$, $i = i^b, ..., i^d$, $m = k = 1, .., N^e_{j_i} - 1$ and for the vertices $l = 3 + j_i$, $i = i^u, ..., i^w$, $m = 1$

$$u^{II}_{3,l,m} = \sum_{i=i^u}^{i^w} \psi_{j_i}(\boldsymbol{\xi}_{l,m}) q^{II}_{3,3+j_i} + \psi^k_{3+j_i}(\boldsymbol{\xi}_{l,m}) q^{II}_{3,9+j_i,k} = 0$$
$$u^{II}_{3,l,m} = \psi_{j_i}(\boldsymbol{\xi}_{l,m}) q^{II}_{3,3+j_i} = 0 \tag{2.19}$$

that gives $\mathbf{k}^{III}\boldsymbol{q}^{II} = \boldsymbol{f}^{III}$

- Backward transformation of the local directions to global ones with $\boldsymbol{q}^{II} = \boldsymbol{\lambda}^{\top}\boldsymbol{q}^{I}$

$$\boldsymbol{\lambda}\mathbf{k}^{III}\boldsymbol{\lambda}^{\top}\boldsymbol{q}^{I} = \boldsymbol{\lambda}\boldsymbol{f}^{III} \tag{2.20}$$

that formally is equivalent to formation of the equation $\mathbf{k}^{IV}\boldsymbol{q}^{I} = \boldsymbol{f}^{IV}$

- Return from generalized DOFs $\boldsymbol{q}^{I}$ to global DOFs $\boldsymbol{q}$ of the element and generation of the final relation

$$\mathbf{k}^{V}\boldsymbol{q} = \boldsymbol{f}^{V} \tag{2.21}$$

2.5. Constrained *hpq*/*hp*-approximation within the elements

Constrained approximation is necessary to enable the connection between elements of different sizes. For that purpose let us divide the element DOFs vector of the smaller element B into two parts corresponding to active and constrained nodes: $\overset{B}{\boldsymbol{q}} = \mathrm{col}[\overset{B}{\boldsymbol{q}}_a, \overset{B}{\boldsymbol{q}}_c]$, and express constrained DOFs through active DOFs of a neighbouring element A of the greater size $\overset{B}{\boldsymbol{q}}_c = \overset{BA}{\mathbf{R}}\,\overset{A}{\boldsymbol{q}}_a$, where $\overset{BA}{\mathbf{R}}$ is the constraint coefficients matrix defined, for triangular-prism elements, by Zboiński and Ostachowicz (1999b). With the above assumptions we can write

$$\overset{B}{\boldsymbol{q}} = \begin{bmatrix} \overset{B}{\boldsymbol{q}}_a \\ \overset{B}{\boldsymbol{q}}_c \end{bmatrix} = \begin{bmatrix} \mathbf{I} & \mathbf{0} \\ \mathbf{0} & \overset{BA}{\mathbf{R}} \end{bmatrix} \begin{bmatrix} \overset{B}{\boldsymbol{q}}_c \\ \overset{A}{\boldsymbol{q}}_a \end{bmatrix} \tag{2.22}$$

where $\mathbf{I}$ is the unity matrix.

Let us take now the equilibrium equation $\overset{B}{\mathbf{k}}{}^{V}\,\overset{B}{\boldsymbol{q}} = \overset{B}{\boldsymbol{f}}{}^{V}$ of element B into consideration and write it according to division of the element nodes into active and constrained ones

$$\begin{bmatrix} \overset{B}{\mathbf{k}}{}^{V}_{aa} & \overset{B}{\mathbf{k}}{}^{V}_{ac} \\ \overset{B}{\mathbf{k}}{}^{V}_{ca} & \overset{B}{\mathbf{k}}{}^{V}_{cc} \end{bmatrix} \begin{bmatrix} \overset{B}{\boldsymbol{q}}_a \\ \overset{B}{\boldsymbol{q}}_c \end{bmatrix} = \begin{bmatrix} \overset{B}{\boldsymbol{f}}{}^{V}_{a} \\ \overset{B}{\boldsymbol{f}}{}^{V}_{c} \end{bmatrix} \tag{2.23}$$

Introduction of the constraint equation (2.22) into the above relation and subsequent left multiplication of (2.23) by transposition of the transformation matrix lead to

$$\begin{bmatrix} \mathbf{I} & \mathbf{0} \\ \mathbf{0} & \overset{BA}{\mathbf{R}}{}^{\top} \end{bmatrix} \begin{bmatrix} \overset{B}{\mathbf{k}}{}^{V}_{aa} & \overset{B}{\mathbf{k}}{}^{V}_{ac} \\ \overset{B}{\mathbf{k}}{}^{V}_{ca} & \overset{B}{\mathbf{k}}{}^{V}_{cc} \end{bmatrix} \begin{bmatrix} \mathbf{I} & \mathbf{0} \\ \mathbf{0} & \overset{BA}{\mathbf{R}} \end{bmatrix} \begin{bmatrix} \overset{B}{\boldsymbol{q}}_a \\ \overset{A}{\boldsymbol{q}}_a \end{bmatrix} = \begin{bmatrix} \mathbf{I} & \mathbf{0} \\ \mathbf{0} & \overset{BA}{\mathbf{R}}{}^{\top} \end{bmatrix} \begin{bmatrix} \overset{B}{\boldsymbol{f}}{}^{V}_{a} \\ \overset{B}{\boldsymbol{f}}{}^{V}_{c} \end{bmatrix} \tag{2.24}$$

The equilibrium equation can now be written in the following blocked form

$$\begin{bmatrix} {}^{B}\mathbf{k}^{V}_{aa} & {}^{B}\mathbf{k}^{V}_{ac}\,{}^{BA}\mathbf{R} \\ {}^{BA}\mathbf{R}^{\top}\,{}^{B}\mathbf{k}^{V}_{ca} & {}^{BA}\mathbf{R}^{\top}\,{}^{B}\mathbf{k}^{V}_{cc}\,{}^{BA}\mathbf{R} \end{bmatrix} \begin{bmatrix} {}^{B}\boldsymbol{q}_{a} \\ {}^{A}\boldsymbol{q}_{a} \end{bmatrix} = \begin{bmatrix} {}^{B}\boldsymbol{f}^{V}_{a} \\ {}^{BA}\mathbf{R}^{\top}\,{}^{B}\boldsymbol{f}^{V}_{c} \end{bmatrix} \tag{2.25}$$

which accounts for constraints of element B due to its connection to larger element A.

3. Adaptive analysis of half-cylindrical moderately thick-shell

In order to prove usefulness of the presented family of the transition elements for modelling and analysis of complex structures, an adaptive analysis of a half-cylindrical, moderately thick shell is performed. The shell has two horizontal clamped edges and two half-cylindrical free edges and is loaded by vertical uniform surface traction $\boldsymbol{p}$ (Fig.2). The thickness of the shell is t, the mid-radius of the shell is R, while the length a of the horizontal and curved edges is the same ($\pi R \approx a$). The thinness ratio t/a equals 3.3%. The admissible value of the total error within elements of the shell was assumed to be less than or equal to 5%.

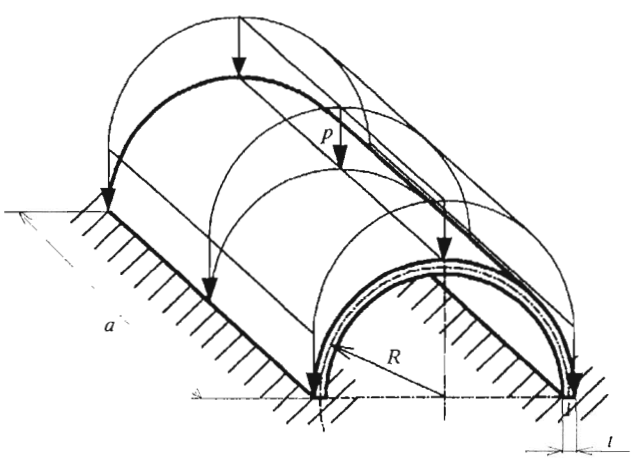

Fig. 2. Half-cylindrical shell geometry and loading

The adaptive FE analysis of the shell consisted of four steps. In each step we carried out global solution for displacements of the structure and then local

solutions within elements leading either to detection of phenomena affecting quality of the solution or error estimation. The first step was performed on an initial mesh which corresponded to uniform, pretty rough mesh for which we applied $h = a/6$, $p = 2$, $q = 1$ and assumed solid elements throughout all the structure. In the second step, modifications of the initial mesh due to improper solution limit and locking phenomena (see Zboiński (1997) for details) are performed. Global adaptive modifications of the *hpq*-mesh performed in this step consisted in assumption of $p = 4$ and change into a Reissner-Mindlin shell model in order to remove locking and improper solution limit, respectively. Note that no changes due to boundary layer phenomena (edge effect) were performed. The reason was the assumed addmissible value of the error. Note that for smaller value of this error such changes could have appeared. The values of the estimated total error within elements of a symmetrical quarter of the shell and the average value of the error are shown in Fig.3. The next two steps (intermediate and final ones) corresponded to local *h*- and *p*-adaptivity, respectively. The final *hpq*-mesh is shown in Fig.4, while the final models applied to the elements are presented in Fig.5. Note that the solid, shell and transition elements were applied within three-dimensional (3D), Reissner-Mindlin (RM), and transition (3D/RM) zones, respectively. The final values of the total errors are displayed in Fig.6.

It can be seen from comparison of Fig.3 and Fig.6 that the change from the modified mesh to the final mesh associated with some model changes within the shell, resulted in decrease of the local maximum error estimate from about 27% to about 7%. At the same time its average value decreased from about 16% to about 2%.

4. Conclusions

Indroduction of the presented family of 3D-based transition elements enables easy connection between 3D-solid and 3D-based Reissner-Mindlin shell finite elements. Thus all parts of the complex structure (solid, shell and transition ones) can be modelled in a consistent way.

Introduction of 3D-based approach and new definition of local, normal and tangent directions as well as application of 3D model and new range of solid and shell parts, facilitate accurate modelling of transition zones of complex structures.

Application of the hierarchical shape functions, assumption of plane strains within shell part of the transition elements, and possibility of imposing con-

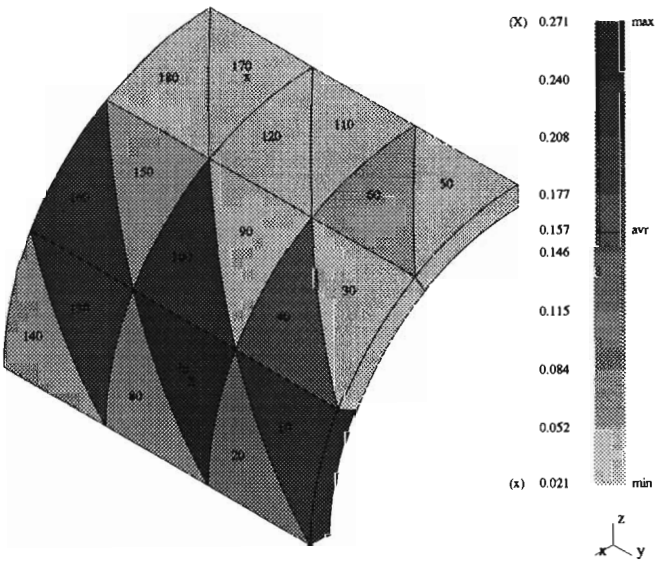

Fig. 3. Local error estimators for the modified mesh of the shell

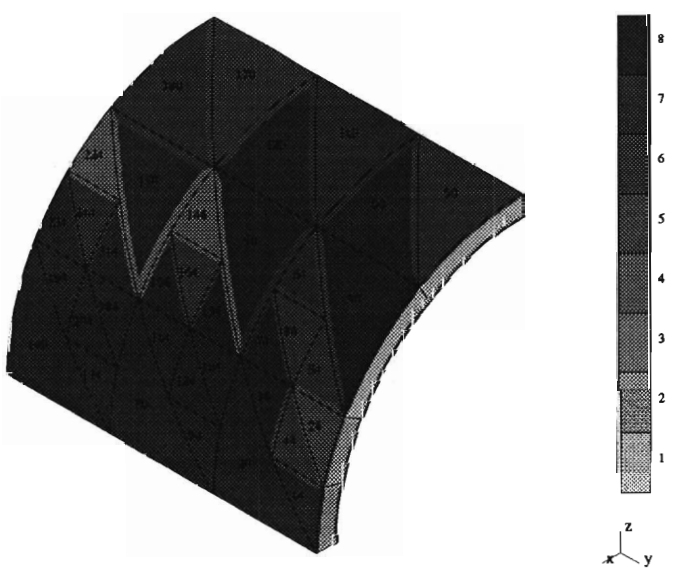

Fig. 4. Final *hpq*-mesh of the analyzed shell

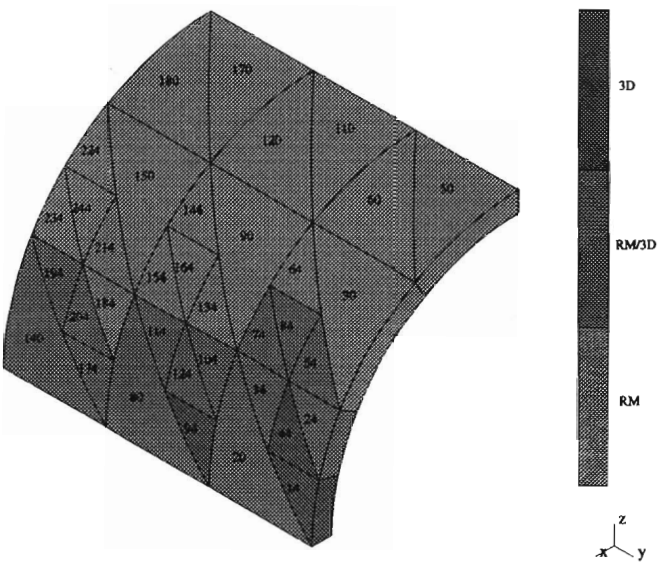

Fig. 5. Models applied within final mesh of the shell

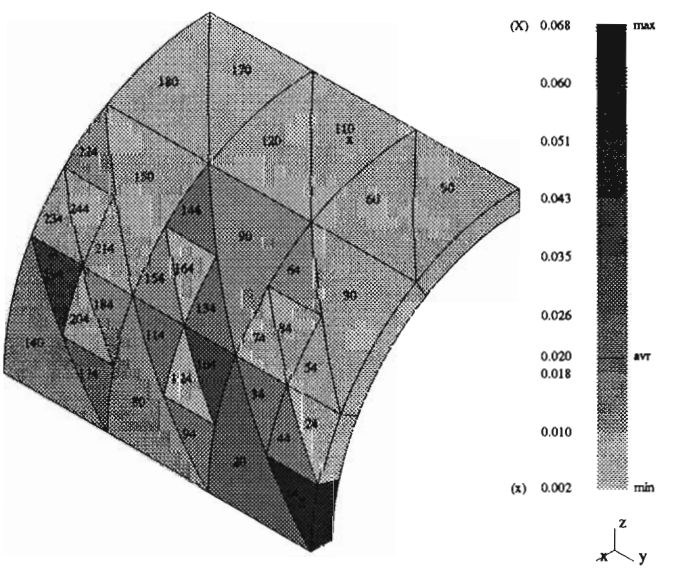

Fig. 6. Local error estimators for the final mesh of the shell

straints corresponding to the transition *hpq*/*hp*-approximations enable connection between elements of different orders of approximation, models, and sizes, respectively. All this leads to very general adaptive strategy for complex structures, which includes model adaptivity as well as *h*-, *p*-, and *q*-adaptivity.

A great potential of the presented family of adaptive solid-to-shell transition elements for modelling and analysis of complex structures has been illustrated by the presented numerical results. Note that joint application of the adaptive solid, shell, and transition elements enables us to diminish the global error of the structure below the assumed value and gives more uniform error distribution within all parts the structure.

References

1. ACTIS R.L., SZABO B.A., SCHWAB C., 1999, Hierarchic Models for Laminated Plates and Shells, *Comp. Meths Appl. Mech. Engng*, **172**, 79-107
2. BABUŠKA I., LI L., 1992, The *hp* Version of the Finite Element Method in Plate Modelling Problem *Comm. Appl. Num. Meths*, **8**, 17-26
3. CHINOSI C., DELLA CROCE L., SCAPOLLA T., 1998, Hierarchic Finite Elements for Thin Plates and Shells, *Computer Assisted Mech. Engng Sciences*, **5**, 151-160
4. DELLA CROCE L., SCAPOLLA T., 1992, High Order Finite Elements for Thin to Moderately Thick Plates, *Computational Mechanics*, **10**, 263-279
5. DEMKOWICZ L., ODEN J.T., RACHOWICZ W., HARDY O., 1989, Towards a Universal *hp* Adaptive Finite Element Strategy, Part 1. Constrained Approximation and Data Structure, *Comp. Meths Appl. Mech. and Engng*, **77**, 79-112
6. ODEN J.T., CHO J.R., 1996, Adaptive *hpq* Finite Element Methods of Hierarchical Models for Plate- and Shell-Like Structures, *Comp. Meths Appl. Mech. Engng*, **136**, 317-345
7. SURANA K.S., 1980, Transition Finite Elements for Three-Dimensional Stress Analysis, *Int. J. Num. Meths Engng*, **15**, 991-1020
8. SZABO B.A., SAHRMANN G.J., 1988, Hierarchic Plate and Shell Models Based on *p*-Extension, *Int. J. Num. Meths Engng*, **26**, 1855-1881
9. ZBOIŃSKI G., 1992, Application of a New Thick Shell Finite Element for Analysis of Long Turbine Blades. *Proc. 17th Int. Seminar on Modal Analysis*, Leuven (Belgium), 977-993
10. ZBOIŃSKI G., 1994, An Adaptive 3D-Based *hp* Finite Element for Plate and Shell Analysis, TICAM Report 95-10, The Univ. of Texas at Austin, Texas

11. ZBOIŃSKI G., 1997, Application of the Three-Dimensional Triangular-Prism *hpq* Adaptive Finite Element to Plate and Shell Analysis, *Computers & Structures*, **65**, 497-514

12. ZBOIŃSKI G., DEMKOWICZ L., 1994, Application of the 3D *hpq* Adaptive Finite Element for Plate and Shell Analysis, TICAM Report 94-13, The Univ. of Texas at Austin, Texas

13. ZBOIŃSKI G., OSTACHOWICZ W., 1995, An Adaptive 3D-Based Solid-to-Shell Transition *hpq/hp* Finite Element, No. 77/97, IFFM, PAS, Gdańsk

14. ZBOIŃSKI G., OSTACHOWICZ W., 1999a, Adaptive Change of Approximation Order, Mesh Density and Model within Complex Structures (in Polish), No. 264/99, IFFM, PAS, Gdańsk

15. ZBOIŃSKI G., OSTACHOWICZ W., 1999b, An Algorithm of Generalized, 3D-Based, *hpq/hp*-Adaptive Transition Element (in Polish), No. 131/99, IFFM, PAS, Gdańsk

Algorytm rodziny opartych na podejściu trójwymiarowym, adaptacyjnych, przejściowych elementów skończonych typu *hpq/hp*

Streszczenie

Praca przedstawia algorytm rodziny nowych, opartych na podejściu trójwymiarowym, pryzmatycznych, adaptacyjnych elementów przejściowych od elementów bryłowych do powłokowych. Elementy oparto na aproksymacjach typu *hpq/hp*, gdzie h, p i q oznaczają średni wymiar elementu oraz wzdłużny i poprzeczny rząd aproksymacji. Istotne *novum* zaproponowanych elementów polega na zastosowaniu w części powłokowej elementu adaptacyjnej aproksymacji typu *hp*, a w części bryłowej adaptacyjnej aproksymacji typu *hpq*. W tym kontekście omówiono dokładniej hierarchiczne funkcje kształtu, modyfikacje macierzy sztywności i wektora sił elementów oraz aproksymacje z więzami. Przydatność elementów w modelowaniu i analizie struktur złożonych potwierdzono zamieszczonym przykładem numerycznym.

Manuscript received March 28, 2000; accepted for print July 25, 2000